Digital microfluidics can also be used in analyses involving biological cells. In a cell-based screen, droplets containing cells, viability reporters, and toxic substrates at different concentrations can be dispensed, mixed, and evaluated with a fluorescence assay (see the figure, middle panel) (*13*). The dose-response curves generated by such devices are more sensitive than equivalent studies on microtiter plates, and cell vitality appears to be unaffected by droplet actuation. Another advantage of digital microfluidics for cell-based assays is the capacity to split and recombine droplets to isolate subpopulations for further analysis (*14*).

Another advantage for the digital microfluidic format is the ease with which electrical components can be integrated into the fluidic circuit. For example, when fabricating an array of droplet-driving electrodes, it is straightforward to also form integrated microheaters for applications that use the polymerase chain reaction. Amplification in such devices can be implemented in half the time and with one-third of the reagent use relative to conventional techniques *(15)*.

As the technology has evolved, the pace of the development of new applications for digital microfluidics has increased. For example, in the past year, Liu *et al*. developed a system for ultra-low–volume DNA ligation (*16*), Luk *et al*. implemented a droplet-based system for proteolytic digestion (*17*), and Fouillet *et al*. reported a technique for carrying out magnetic-bead–based sample processing (*18*). In addition to new applications, there is a regular stream of innovations in digital microfluidic device infrastructure. For example, Chiou *et al*. recently reported the capacity to optically actuate "virtual electrodes," which allows for much greater flexibility in device geometry and design (*19*). Likewise, Abdelgawad *et al*. recently demonstrated digital microfluidic processes on open, nonplanar substrates, which facilitates integration of different physicochemical environments on a common platform (see the figure, right panel) (*20*).

The capacity to use electricity to control the shape and position of droplets on surfaces has led to a dynamic new field of research. Taking a cue from the lotus leaf and the *Stenocara* beetle, we are learning to put surface energies to work, in applications ranging from optics to laboratory miniaturization. Given the trajectory of innovation in this field, it is likely that this work has only just begun.

References

1. X. M. Li *et al*., *Chem. Soc. Rev.* **36**, 1350 (2007).
2. M. G. Pollack *et al*., *Appl. Phys. Lett.* **77**, 1725 (2000).
3. J. Lee *et al*., *Sens. Actuators* **A 95**, 259 (2002).
4. B. Berge, J. Peseux, *Eur. Phys. J.* **E 3**, 159 (2000).
5. L. Hou *et al*., *Appl. Phys. Lett.* **90** (2007).
6. Varioptic, www.varioptic.com.
7. Philips, www.research.philips.com/technologies/light_dev_microsys/fluidfocus.
8. D. Chatterjee *et al*., *Lab Chip* **6**, 199 (2006).
9. M. Abdelgawad, A. R. Wheeler, *Adv. Mater.*, 10.1002/adma.200802244, in press.
10. E. M. Miller, A. R. Wheeler, *Anal. Bioanal. Chem.*, 10.1007/s00216-008-2397-x, in press.
11. A. Huebner *et al*., *Lab Chip*, **8**, 1244 (2008).
12. E. M. Miller, A. R. Wheeler, *Anal. Chem.* **80**, 1614 (2008).
13. I. Barbulovic-Nad *et al*., *Lab Chip* **8**, 519 (2008).
14. S. K. Fan *et al*., *Lab Chip* **8**, 1325 (2008).
15. Y.-H. Chang *et al*., *Biomed. Microdevices* **8**, 215 (2006).
16. Y.-J. Liu *et al*., *J. Micromechan. Microeng.* **18**, 045017 (2008).
17. V. N. Luk, G. C. Mo, A. R. Wheeler, *Langmuir* **24**, 6382 (2008).
18. Y. Fouillet *et al*., *Microfluid. Nanofluid.* **4**, 159 (2008).
19. P. Y. Chiou *et al*., *J. Microelectromechan. Syst.* **17**, 133 (2008).
20. M. Abdelgawad *et al*., *Lab Chip* **8**, 672 (2008).

10.1126/science.1165719

GEOLOGY

The Story of O_2

How did biological, geochemical, and geophysical processes produce an atmosphere that allowed complex animal life to evolve?

Paul G. Falkowski[1] and Yukio Isozaki[2]

Two gases overwhelmingly dominate Earth's atmosphere: N_2 and O_2. The former is primordial, and its presence and abundance are not driven by biological processes. Indeed, N_2 is virtually inert and has an atmospheric lifetime on the order of 1 billion years (*1*). In contrast, O_2 is continuously produced biologically via the oxidation of water driven by energy from the Sun. The gas was almost certainly virtually nonexistent in Earth's early atmosphere, is highly reactive, and has an atmospheric lifetime of ~4 million years (*2*). Yet despite this comparatively short atmospheric lifetime, O_2 came to constitute ~10 to 30% of the atmospheric volume for the past ~500 million years (*3*, *4*).

How did O_2, a gas critical to the evolution of animal life, become the second most abundant gas on Earth? The story is not as simple as it might first appear (*5*, *6*). To understand it, we must know not only how and when O_2 was first generated, but also how it came to persist in high concentrations in the atmosphere.

Elemental oxygen (O) is produced via the so-called "main line" nuclear reaction sequence from successive ^{4}He fusion reactions in hot stars. It was delivered to the early Earth chemically bound to other elements. Through successive cycles of heating and cooling, O reacted with Si and C to form two of the major anions that, together with metal cations, constitute the fundamental minerals in mantle and crust, and with H to form water (*7*). Additional water was delivered to the planetary surface via meteorites and possibly comets; however, the relative proportions of the three sources are not well known (*8*). Regardless of the source, isotopic data suggest that Earth's surface contained liquid water within ~200 million years after the accretion of the planet (*9*). Liquid water is a necessary condition for life as we know it, but it is not a sufficient condition for the biological production of O_2.

Although water can be oxidized to its component elements by ultraviolet light, this reaction can produce only extremely small concentrations of O_2 because of strong negative feedbacks (*10*). The overwhelming source of O_2 on Earth is photobiological oxidation of water; neither the evolution nor the mechanism of this process are completely understood (*11*, *12*). Apparently it arose once in a single clade of bacteria and was then appropriated via a single event, in which one cell engulfed another (endosymbiosis) to form a new symbiotic organism. The latter became the progenitor of all photosynthetic eukaryotes, including algae and higher plants (*12*).

The core of the oxidation machinery is photosystem II, a large protein complex containing four manganese atoms that are photocatalytically oxidized to create electron holes upstream. O_2 is produced as a waste product via the reaction

$$2H_2O \rightarrow 4e + 4H^+ + O_2$$

The protons and electrons generated are used to reduce CO_2 to form organic matter via

$$CO_2 + 4e + 4H^+ \rightarrow (CH_2O) + H_2O$$

[1]Department of Earth and Planetary Sciences and Institute of Marine and Coastal Sciences, Rutgers University, 71 Dudley Road, New Brunswick, NJ 08901, USA. [2]Department of Earth Science and Astronomy, University of Tokyo, 3-8-1 Komaba, Meguro, Tokyo 153-8902, Japan. E-mail: falko@imcs.rutgers.edu; isozaki@ea.c.u-tokyo.ac.jp

On time scales of years to millennia, these reactions are closely coupled to the reverse process of respiration, such that net production of O_2 is virtually nil. That is, without burial of organic matter in rocks, there would be very little free O_2 in the atmosphere. Hence, the evolution of oxygenic photosynthesis was a necessary but not a sufficient condition to oxidize Earth's atmosphere.

Net oxidation of the atmosphere requires long-term storage of the reductants, primarily as organic carbon. The largest reservoir, by far, is Earth's crust. The major mechanism for burial of organic matter is sedimentation and accretion onto cratons (stabilized continents) and, to a lesser extent, subduction deep into the mantle (see the figure). These processes are driven by plate tectonics, in which radiogenic heat in Earth's interior drives mantle convection, allowing continents to collide and separate to form new ocean basins. During these cyclical collisions and separations, oceanic plates are eventually subducted under continents, and a fraction of the organic matter buried in the sediments is tectonically added to the continent, forming coastal mountain belts and thus increasing continental mass. Indeed, unless a large fraction of the organic matter stored in marine sediments is stabilized in cratons, it will be subducted, heated, and in part recharged to the atmosphere via volcanism, where it would become reoxidized (*13*, *14*).

Thus, burial of organic matter, which contains reducing equivalents derived from the biological oxidation of water, implies a net oxidation of the atmosphere. The presence of O_2 in the atmosphere requires an imbalance between oxygenic photosynthesis and aerobic respiration on time scales of millions of years; hence, to generate an oxidized atmosphere, more organic matter must be buried than respired.

How well do we know the concentration of O_2 in Earth's atmosphere over geological time? Perhaps surprisingly, not very well. The major tool for quantitative reconstruction of the oxidation state of the planet is based on isotopic analysis of carbon in carbonates, and, to a lesser extent, sulfur in various mineral phases (*3*). Photosynthetic carbon fixation strongly discriminates against $^{13}CO_2$, such that the resulting organic matter is enriched in $^{12}CO_2$ relative to the source (mantle) carbon. In contrast, carbonates, formed by the precipitation of HCO_3^- in seawater with Ca^{2+} and Mg^{2+}, retain the isotopic signal of the source carbon. If photosynthesis exceeds respiration (implying burial of organic carbon), ^{12}C is removed from the mobile pool of carbon in the atmosphere and oceans, leaving a ^{13}C-enriched carbon source for biological and geochemical processes. Thus, the isotopic composition of carbon in carbonates can be used to track the extent to which organic matter was buried and was returned to the mobile pools over geological time (*3*, *15*).

Although the initial oxidation of the atmosphere appears to have occurred about 2.2 billion years ago, atmospheric O_2 concentrations were probably ~1% of the present atmospheric level or less, and the deep ocean was likely still anoxic (*16*, *17*). Large increases in atmospheric O_2 appear to have occurred much later in Earth history, in the late Neoproterozoic (~750 to 550 million years ago) and the Carboniferous (360 to 300 million years ago).

The boost in O_2 inferred in the Neoproterozoic, inferred from carbon isotopic data, corresponds biologically to a rise in ecological prominence of large, single-celled eukaryotic algae (*12*)—that is, phytoplankton—which would have greatly accelerated the burial of organic matter in marine sediments, as well as geophysical controls resulting from mantle cooling and enhanced subduction. Metamorphic rock records through history suggest that heat flow from Earth's interior decreased steadily as the planet gradually cooled, and the geothermal gradient reached a threshold where hydrous (OH-containing) minerals were subducted deeper into the mantle (*18*). This process would have led to a massive transfer of surface water into mantle, potentially accelerating the extensive emergence of continents. This hypothesis is further supported by the historical record of oxygen isotopes (*19*).

The burial of large amounts of organic carbon over the past 750 million years is mirrored in a substantial rise in atmospheric O_2, which may have triggered the Cambrian explosion of animal life (*18*, *20*). Further increases in burial efficiency were accelerated in the Carboniferous (350 to 300 million years ago), as land plants, especially trees, came to double the primary productivity of the planet (*3*). Indeed, models based on the isotopic record of carbon and sulfur suggest that this period of Earth's history witnessed O_2 concentrations as high as ~30% (*3*). A very small fraction of the buried marine and terrestrial carbon was preserved as natural gas, petroleum, and coal. Currently, humans extract these resources at a rate about 1 million times the rate at which they were deposited in the lithosphere.

By the end of the Triassic extinction, O_2 concentrations appear to have been much lower (*21*), perhaps even as low as 10 to 12% (*3*, *4*).

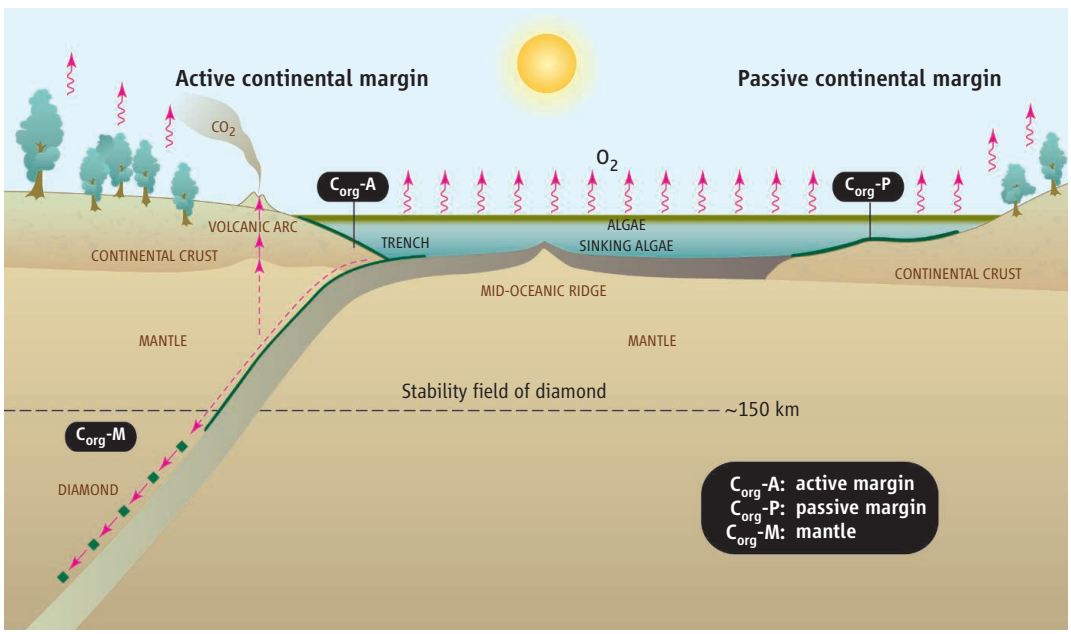

Processes controlling the flux and accumulation of O_2 on Earth. Water is photobiologically split with solar energy by algae in the ocean and plants on land. A very small fraction of the organic matter produced by these organisms is buried in sediments, and ultimately tectonically added to continents and subducted deep into Earth's mantle, thereby permitting O_2 levels to accumulate in the atmosphere. The balance between burial of organic matter and its oxidation appears to have been tightly controlled over the past 500 million years.

CREDIT: ADAPTED BY P. HUEY/*SCIENCE*

Published by AAAS

Over the past 200 million years, O_2 concentrations have varied from ~10% at the low end to as much as 23% at the high end (*4*). The relatively narrow range of variability suggests tight controls on the rate of burial and oxidation of organic matter on Earth's surface. Indeed, existing data do not show a long-term nonperiodic increase in ^{13}C in carbonates over the past 2 billion years, implying that the reservoir of inorganic carbon in Earth's mantle is extremely large relative to the fraction of organic carbon buried, and that the burial of organic carbon is roughly balanced by oxidation and weathering.

This brief exploration shows that we understand in broad terms how O_2 came to form a substantial part of Earth's atmosphere, but many details remain sketchy. We still do not understand the mechanism responsible for water splitting in oxygenic photosynthesis, nor do we know what controls the concentration of the gas in our planetary atmosphere (*6*, *13*). The former issue should be resolved within a decade with the aid of high-resolution structures of the photosystems and sophisticated biophysical approaches to measuring electron transfer reactions (*22*). The latter issue will be more difficult to constrain, but a better understanding will emerge from more complete models coupled with better-integrated biogeochemical measurements (*15*).

Each mole of oxygen in Earth's atmosphere required ~450 kJ equivalents of photon energy to produce. Given a concentration of $\sim 4 \times 10^{19}$ moles of O_2 in the contemporary atmosphere, the reservoir of the gas represents a staggering 2×10^{10} TJ hydrogen bomb equivalents of energy that is replaced every ~4 million years. Nature certainly has provided an incredible source of potential energy for the evolution of life on Earth.

References

1. R. A. Berner, *Geology* **34**, 413 (2006).
2. R. F. Keeling *et al.*, *Global Biogeochem. Cycles* **7**, 37 (1993).
3. R. A. Berner, *The Phanerozoic Carbon Cycle: CO_2 and O_2* (Oxford Univ. Press, New York, 2004).
4. P. G. Falkowski *et al.*, *Science* **309**, 2202 (2005).
5. D. C. Catling, M. W. Claire, *Earth Planet. Sci. Lett.* **237**, 1 (2005).
6. L. R. Kump, *Nature* **451**, 277 (2008).
7. H. D. Holland, *The Chemical Evolution of the Atmosphere and Oceans* (Princeton Univ. Press, Princeton, NJ, 1984).
8. F. Robert, *Science* **293**, 1056 (2001).
9. S. Mojzsis *et al.*, *Nature* **409**, 178 (2001).
10. J. Kasting, J. Walker, *J. Geophys. Res.* **86**, 1147 (1981).
11. R. E. Blankenship, *Photosyn. Res.* **33**, 91 (1992).
12. P. G. Falkowski, A. H. Knoll, Eds., *Evolution of Primary Producers in the Sea* (Academic Press, San Diego, CA, 2007).
13. P. G. Falkowski, L. Godfrey, *Philos. Trans. R. Soc. London Ser. B* **363**, 2705 (2008).
14. R. Tappert *et al.*, *Geology* **33**, 565 (2005).
15. J. M. Hayes, J. R. Waldbauer, *Philos. Trans. R. Soc. London Ser. B* **361**, 931 (2006).
16. D. E. Canfield, *Nature* **396**, 450 (1998).
17. D. E. Canfield, *Annu. Rev. Earth Planet. Sci.* **33**, 1 (2005).
18. S. Maruyama, J. Liou, *Int. Geol. Rev.* **47**, 775 (2005).
19. J. Jaffres *et al.*, *Earth Sci. Rev.* **83**, 83 (2007).
20. A. H. Knoll, S. B. Carroll, *Science* **284**, 2129 (1999).
21. Y. Isozaki, *Science* **276**, 235 (1997).
22. J. Barber, A. Rutherford, Eds., *Philos. Trans. R. Soc. London Ser. B* **363**, 1125 (2008).

10.1126/science.1162641

MEDICINE

Can We Nip Obesity in Its Vascular Bud?

The origin of fat tissues and identity of factors that direct fat development in animals are becoming more clear.

C. Ronald Kahn

Almost all animal species store energy in the form of fat. The worm *Caenorhabditis elegans* stores fat in intestinal epithelium, and sharks store fat in the liver, but most animal species store fat in white adipose tissue (*1*). In normal-weight adult humans, white adipose tissue represents 10 to 29% of body weight, making fat the largest organ in the body. Moreover, fat mass increases in obesity, and we are in the midst of a worldwide epidemic of obesity. Indeed, two-thirds of the U.S. population and more than 1 billion people worldwide are either overweight or obese. As a result, obesity-related pathologies, such as diabetes, cardiovascular disease, imbalances in lipid metabolism (dyslipidemias), and fatty liver (hepatic steatosis) have surpassed tobacco use as a cause of death. Although we have a detailed understanding of how preadipocytes differentiate into adipocytes (fat cells), very little is known about the origin of preadipocytes. On page 583 in this issue, Tang *et al.* (*2*) show that the precursor cells that give rise to white adipocytes reside within the walls of the blood vessels that supply adipose tissue.

Adipose tissue is generally thought to originate from the mesoderm (*1*). In this model, embryonic mesoderm gives rise to mesenchymal stem cells, which in turn give rise to common early precursors or adipoblasts. Under appropriate conditions, adipoblasts develop into committed white and brown preadipocytes and ultimately mature adipocytes (see the figure). However, there are no unique molecular markers expressed by preadipocytes, and thus the exact nature of these precursors, the specific steps in lineage commitment and differentiation, and the factors controlling these pathways are not clear. Tang *et al.* used lineage tracing in mice to show that the precursor cells that give rise to white adipocytes are pericytes, smooth muscle–like cells that cover the endothelial cells of blood vessels. These specialized cells express the proteins peroxisome proliferator-activated receptor γ (PPARγ), stem cell antigen 1 (sca1), and CD34. This cell population also expresses smooth muscle actin (SMA), platelet-derived growth factor receptor–β (PDGFR-β), and neural/glial cell 2 (NG2), which are all markers of pericytes, but not perilipin, a marker of mature adipocytes. Previously, the only known marker of preadipocytes was Pref-1 (also known as DLK-1), a cell surface protein in the epidermal growth factor family (*3*). However, Pref-1 is not unique to the preadipocyte and is unsuitable for isolation or tracking of these cells.

The findings of Tang *et al.* support previous work in mice showing that when the stromovascular fraction of adipose is analyzed by flow cytometry (a technique that examines individual cells for physical and molecular characteristics), preadipocytes are enriched in the fraction of cells that express the cell surface protein CD34 but not CD31 (*4*, *5*), and that the vascular supply to fat can be rate limiting in the accumulation of adipose (*6*). Although Tang *et al.* find the PPARγ-expressing cells only in blood vessels that supply adipose tissue, pericytes isolated from other locations have adipogenic, myogenic, osteogenic, and chondrogenic potential (*7*), with the switch between fates controlled in part by developmental signals (such as Wnt) and growth factor signaling.

Multipotent stem cells can also be isolated from adipose stromovascular fraction and

Joslin Diabetes Center, One Joslin Place, Boston, MA 02215, USA. E-mail: c.ronald.kahn@joslin.harvard.edu